Proceedings of NAWTEC16
16th Annual North American Waste-to-Energy Conference
May 19-21, 2008, Philadelphia, Pennsylvania, USA

NAWTEC16-1949

CO_2 Enhanced Steam Gasification of Biomass Fuels

Heidi C. Butterman and Marco J. Castaldi*
Department of Earth and Environmental Engineering (HKSM)
Columbia University, New York, N.Y. 10027

Abstract

The current study involves an experimental investigation of the decomposition of various biomass feedstocks and their conversion to gaseous fuels such as hydrogen. The steam gasification process resulted in higher levels of H_2 and CO for various CO_2 input ratios. With increasing rates of CO_2 introduced into the feed stream, enhanced char conversion and increased CO levels were observed. While CH_4 evolution was present throughout the gasification process at consistently low concentrations, H_2 evolution was at significantly higher levels though it was detected only at elevated gasification temperatures: above 500^o C for the herbaceous and non-wood samples and above 650^{o}C for the wood biomass fuels studied.

The biomass feedstocks were studied through the use of Thermo Gravimetric Analysis (TGA), Gas Chromatography, Calorimetry, Atomic Absorption Spectrophotometry (AAS), and the Scanning Electron Microscope with Energy Dispersive X-Ray Analysis (SEM/EDX). The chemical composition of the various biomass fuels and their combustion and gasification ash residues, in addition to the mass decay and gaseous evolution behavior were investigated as a function of temperature.

The thermal treatment of biomass fuels involves pyrolysis and gasification with combustion occurring at the higher temperatures. In the gasification environment, when combustion processes are occurring, gaseous components evolve from the fuel and react with oxygen either released from the biomass structure itself, or from the injected steam and CO_2. These high temperature reactions are responsible for the enhanced burnout of the carbon (charcoal) structure that is produced during the low temperature pyrolytic breakdown of the biomass. Since the ligno-cellulosic biomass component typically found in U.S. MSW is greater than 50%, techniques to enhance the thermal treatment of biomass feedstocks can also aid in the processing of MSW.

Gas evolution as a function of temperature was monitored for H_2, CH_4, CO_2 and CO for several biomass fuels that included woods, grasses and other ligno-cellulosic samples. These included oak, sugar maple, poplar, spruce, white pine, Douglas fir, alfalfa, cordgrass, beachgrass, maple bark, pine needles, blue noble fir needles, pecan shells, almond shells, walnut shells, wheat straw, and green olive pit. The TGA mass decay curves showed similar behavior for the woods, grasses and agricultural residues, where most of the mass loss occurred before 500oC. Most feedstocks exhibited 2 constant mass steps though several exhibited a third with completed mass loss by 900^o-1000^{o}C. Two distinct mass decay regimes were found to correlate well with two distinct gas evolution regimes exhibited in the curves for CO, H_2 and CH_4. Most of the mass loss occurred during pyrolysis, with the remaining degradation to ash or char occurring in the high temperature gasification regime.

One characteristic of biomass samples is the highly variable nature of the mineral composition. SEM/EDX analyses indicated high levels of potassium, magnesium and phosphorus in the ash residue. The devitrification and embrittlement of the quartz furnace and balance rods were attributed to the high mineral content of many of the biomass feedstocks, with the high alkaline oxide levels of the grasses being particularly destructive. While mineral content may exert a beneficial effect through enhanced char reactivity with the possibility for a more thorough processing of the feedstock, the potential for corrosion and slagging would necessitate the judicious selection and possible pretreatment of biomass fuels. A major advantage of thermal treatment through gasification prior to combustion is the ability to remove many of the corrosive volatiles and ash elements such as potassium, sodium and chlorine to avert damage to the process equipment.

1. Introduction

Rising energy demands, heightened awareness of man's impact on the global climate system, and the inherent instability of energy geopolitics have led to a greater awareness of the importance of developing sources of energy that can either augment the capacity or replace the use of fossil fuels. One of the more promising renewable energy sources is biomass fuels. They can address both energy security and, being a carbon neutral energy source, environmental sustainability and corporate accountability. Though currently less than 3% of the U.S. energy production is through the use of renewable energy sources, about one third of this

Copyright © 2008 by ASME

is attributable to woods, grasses, forestry wastes and agricultural residues. Biomass feedstock capacity has been calculated as having the potential to supply 5% of the nation's power by 2030, while biomass derived fuels offer even more promise in being able to meet 20% of the domestic transportation demand (1). Current energy studies predict a doubling of energy consumption within the next 30-40 years. Heightened public awareness of the burning of fossil fuels and their connection to visible evidence of climate change has led to legislation limiting CO_2 emissions that have far reaching impact in the industrial, commercial and public sectors.

As energy productivity, efficiency and supply become more critical to economic viability and as global emissions standards become more stringent, the capabilities of existing technologies will need to evolve to meet more demanding engineering constraints. Sustainability and energy security will drive engineering designs to incorporate more efficient processes and equipment. These designs will strive to meet a zero emission energy conversion policy as we head towards a zero waste atom economy. Companies currently engaged in energy intensive industries are looking at renewable resources technologies that will enable them to be more energy efficient and economically competitive. Many of these companies, such as those in the lumber industry, have chosen gasification technology for wood residue-to-energy and see the operational shift as a long term strategic investment.

Globally, economic factors have driven the use of indigenous fuels to satisfy the need for power and energy in emerging economies. Biomass has taken a more prominent role for use as transportation and industrial fuels in addition to the traditional use for household cooking and light. In these developing nations, use of biomass as cooking fuel in combination with cooking stove technology transfer has led to decreased particulate emissions and indoor CO levels, a corresponding decreased incidence of respiratory infection and more sustainable local economies. Emerging economies have been considering the alternative use of various biomass sources as fuel rather than food, and the importance of land preservation initiatives that couple biomass harvesting with sustainable agroforestry. Policy formulation that includes education of individuals in these emerging economies is essential. They need to be made aware of the benefits of alternatively using biomass residues as fuel to support sustainable energy production rather than exclusively for traditional soil nutrient replenishment.

Pollutants from combustion and their atmospheric transport is a very active research topic in the field of climatological modeling. Gasification, rather than combustion, offers the opportunity to control the level of these gaseous and particulate emissions leading to lower concentrations of soot particles and aerosols. The soot created from the combustion of diesel, coal and wood fuels results in both positive dark particle warming and negative shiny particle cooling of the atmosphere. Particulate transport and atmospheric chemistry as well as aerosol emissions need to be considered when developing regional and global scale climate models. Biomass-burning aerosols were observed to be more easily precipitated over Africa than other continents such as South America. This finding, coupled with the fact that Africa produces most of the global biomass burning emissions, is essential in developing local climate models. Heightened concern for the consequences of global warming and the consequences of regionally produced but globally dispersed pollutant transport has led to technology transfer to developing nations. This has enabled them to more efficiently combust fuels or is currently helping them to find alternative means, such as gasification technology, to produce adequate supplies of energy, power and heat in an economically viable and environmentally sustainable way, that would ultimately be globally beneficial.

Compared to a typical fossil fuel, the complex ligno-cellulosic structure of biomass is more difficult to gasify or combust. The nature of the mineral impurities in conjunction with the presence of various inorganic species, as well as sulfur and nitrogen containing compounds, adversely impacts the benign thermal processing of the oxygenated hydrocarbon structure of the biomass. While combustion of biomass feedstocks results in fuel-bound nitrogen and sulfur being converted to NO_x and SO_x , steam gasification involves thermal treatment under a reducing atmosphere resulting in fuel-bound nitrogen release as N_2 and fuel-bound sulfur conversion to H_2S that is more easily removed by means of adsorption beds. Unlike combustion, the gasification process is more energy intensive. Careful engineering of the process is necessary if the result is to produce rather than consume a significant amount of energy or power as a result of the thermal treatment.

Introduction of steam as a reactant influent durng gasification has been shown to enhance H_2 production during the gasification of a variety of fuels that include coal, biomass, and municipal solid waste (2, 3, 4). Introduction of CO_2 has been shown (5) to enhance the CO production during high temperature steam gasification while depressing the H_2 and CH_4. Both the steam and CO_2 have been shown to increase the char reactivity (6,7,8) through a modification of the char pore structure and surface activity. Biomass gasification using steam can result in increased H_2 concentration in the synthesis gas with higher concentrations corresponding to higher gasification temperatures in the 700-1100^oC range. If a CH_4 fuel stream is the preferred product then careful monitoring of the process to operate below 600^oC would permit optimizing CH_4 production while minimizing the H_2 stream. A general

Copyright © 2008 by ASME

characteristic of the fuel stream produced through gasification is a clean stream with a minimum of tar, soot and particulates. Biomass gasification results in a producer gas whose main components are CO, H_2 and CH_4. Other volatile components include CO_2, acetaldehyde, acetic acid, phenol, formaldehyde, formic acid and acetone. Since the gasification process was performed under high levels of N_2 dilution, many of these species were not detectable since they were present in the parts per million range.

At gasification temperatures in the 700-1200°C range, the dominant reactions that govern biomass steam gasification are the steam reforming reaction

$$C + H_2O \rightarrow CO + H_2$$
$$\Delta H = +131.3 \text{ kJ/mol}, \quad (1)$$

and the Boudouard reaction

$$C + CO_2 \rightarrow 2CO$$
$$\Delta H = +172.5 \text{ kJ/mol}, \quad (2)$$

in addition to the pyrolytic cleavage and condensation reactions that break down the biomass lattice structure, the decomposition reactions of the oxygenated minerals releasing O_2, the oxidation of the char

$$C + \tfrac{1}{2} O_2 \text{ (from biomass structure)} \rightarrow CO$$
$$\Delta H = -110.5 \text{ kJ/mol}, \quad (3)$$

and the reverse water gas shift reaction (RWGS)

$$H_2 + CO_2 \rightarrow CO + H_2O$$
$$\Delta H = +41.2 \text{ kJ/mol}, \quad (4)$$

to release CO and CO_2 as the char degrades from a hydrocarbon skeleton to a mineral ash residue. Though H_2 evolution appeared to commence for many runs shortly after 500°C, a pronounced depression in the H_2 concentration was not clearly discernable until after 700°C. A measurable enhancement of CO evolution with CO_2 recycle and a pronounced increase in CO concentration due to the Boudouard reaction was observed for all feedstocks. The strongest signal appeared following pyrolysis in the gasification regime. At much higher gasification temperatures above 1050°C, H_2 dissociation competes with H_2 formation tending to decrease the net yield of molecular H_2. Many of the rapid drops in gas evolution concentrations were attributable to the exhaustion of biomass at the high temperatures, particularly for the higher CO_2 ratios. Characteristically different CH_4 behavior was observed for the woods and grasses as compared to the agricultural residues. While the optimum methane production for the wood and herbaceous feedstocks occurred in the interval between 500-600°C, that for the residues occurred between 600-800°C with a significantly higher value for the residue CH_4 mole fraction. The lignin and cellulose structural components of biomass feedstocks each have their own collection of characteristic mechanisms whose reactions are coupled and influenced by the mineral impurities and the interaction of the CO_2 with the thermal decomposition products. The thermodynamically favored products of steam gasification at these elevated temperatures are CO and H_2. Biomass fuels high in lignin content were observed to produce higher char yields following pyrolysis up to about 450°C. Through subsequent thermal treatment at elevated temperatures, enhanced production of gaseous products was possible through injection of H_2O and CO_2. This improved tar and char conversion to volatiles translates to economic and environmental advantages through less waste residue for treatment and minimization of highly alkaline ash residue responsible for corrosive damage to the process equipment. Large ash volume due to oxidized minerals more prevalent in the grassy feedstocks, when subjected to the high gasification temperatures, can lead to melting and agglomeration and thus slagging as a result of thermal treatment.

Biomass feedstocks offer the promise of new sustainable sources for chemicals, energy and power. Nevertheless, the great variability in chemical composition results in a wide variety of gas evolution profiles, heat content, and potential for corrosive behavior. Through the use of Gas Chromatography, Thermogravimetric Analysis and Scanning Electron Microscopy with Energy Dispersive X-Ray Analysis, along with chemical information that can characterize the distribution of ligno-cellulosic structural components, we have begun to interpret the gas evolution as a function of composition, mass decay and temperature. Ultimately a better understanding of the thermal processing of the various biomass fuels will result in a more informed prediction as to the energy production potential for the various feedstocks. The current study examined CO_2 injection as a technique to enhance char burnout by creating more reactive chars that result in more complete thermal treatment. Thermal processing techniques that can more completely convert biomass fuels are transferable to MSW processing since more than half of the mass of municipal waste is biogenic in origin.

2. Experimental Setup

2.1 Gasification System. Figure 1 shows a schematic diagram of the gasification test facility in the Castaldi Combustion and Catalysis Lab at Columbia University, Henry Krumb School of Mines. It consists of an Instrument Specialists Temperature Programmer Interface/Thermal Analyzer that, through Acquisition software, can

Copyright © 2008 by ASME

regulate the temperature and heating rate of the quartz furnace in the Dupont 951 Thermogravimetric Analyzer. The carrier flow consists of UHP N_2 and Bone Dry CO_2 whose flow rates are regulated by means of two Gilmont GF 1060 rotameters. A kd-Scientific 780-100 syringe pump feeds distilled water into a stainless steel steam generator that produces slightly superheated steam (~110─120^{o}C) whose temperature is monitored by an Omega digital E-type thermocouple readout prior to entering the furnace. The total feed flow (steam + N_2 + CO_2) was maintained at 90 mL/min. The volumetric % CO_2 fed into the line varied from 0-50% while the level of water introduced was kept at room temperature saturation values. Gaseous steam was introduced into the furnace by means of a side arm through which flowed the steam and that portion of the N_2 and CO_2 remaining after a fraction was diverted for purge flow to prevent deposition onto the TGA electronics. The gasification process was run with excess H_2O and CO_2 to ensure that the biomass was the limiting agent in the steam gasification reactions.

The biomass sample sits in an inert platinum pan suspended on either a quartz or ceramic rod. Gas evolution data is recorded as a function of temperature with the mass decay as a function of temperature displayed graphically in real time on the TPI/TGA Acquisition software. Text files are exported to a spreadsheet for processing. The incoming reactants and biomass products of gasification exit the furnace and enter an ice-water condensation column that removes any moisture from the gas evolution products prior to entering the Agilent 3000A micro-gas chromatograph. The carrier gases for the 4-channel micro-GC are UHP He and UHP Ar. The chromatograph sensitivity and resolution is in the single digit ppm V range. The GC chromatograms are generated by Agilent Cerity software and the data is stored in a spreadsheet for processing.

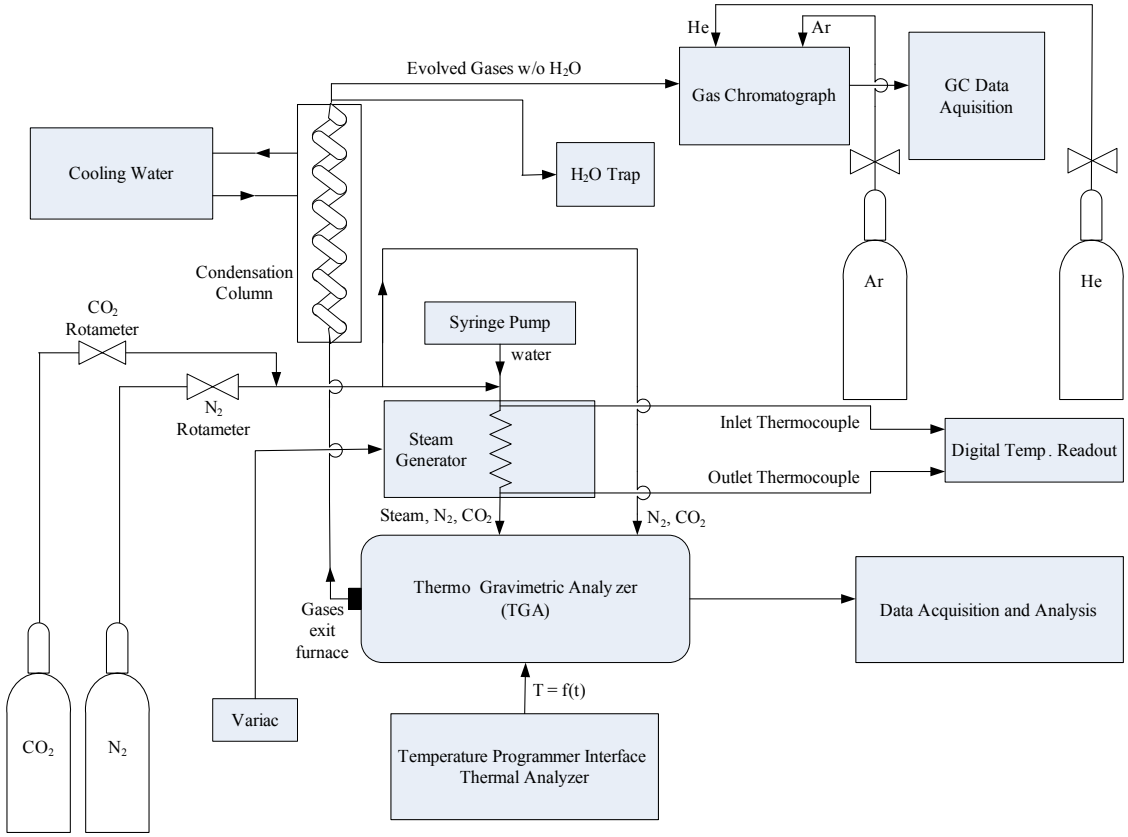

Figure 1. Schematic of experimental apparatus

2.2 Methodology of Gasification Testing. The wood samples were prepared by drilling cores within planks of untreated wood to produce dry sawdust. The herbaceous feedstocks were air-dried, ground by mortar and pestle and then ball-milled. The amount of mechanical processing was done so as to minimize the chemical degradation of the feedstock. Evidence

Copyright © 2008 by ASME

of this degradation could be seen in the distinctly different gas evolution profiles exhibited by the green pine needles as compared to the dried pine needles. None of the grasses or needles were water washed but used as received to maintain the original mineral content of the sample. Only the beachgrass sample needed careful inspection and pretreatment so that it could be cleaned of all sand grains. All of the residue samples, shells and pits, were pulverized with a coarse drill bit while the rice hulls were ground with mortar and pestle.

The feedstocks included spruce, white pine, Douglas fir, poplar, sugar maple, oak, alfalfa, cordgrass, American beachgrass, pine needles, maple bark, blue noble fir needles, wheat straw, green olive pit, pecan shell, almond shell, walnut shell, peanut shell, rice hull and cotton plant. The typical size of the samples ranged from 20-25 mg. The agricultural residues gas evolution runs used samples that were 27-30 mg. The Douglas fir sample was 16 mg, poplar was 25 mg, beachgrass was 34 mg and the large pan beachgrass sample was 110 mg. The samples have their weight both measured in real time by the TPI/TA software and, for verification, each sample is weighed on a Mettler scale accurate to +/- 0.1mg.

The total incoming flow of CO_2+N_2+H_2O is maintained at 90 mL/min, with the syringe pump regulating the distilled water flow rate, and rotameters regulating the bone dry CO_2 and UHP N_2 rates so as to maintain the desired CO_2 concentration. The relatively small sample in the TGA pan and the relatively high flow rate of the feed result in significant dilution of the gas evolution products detected by the mico-GC. To more clearly identify H_2, Ar is used as the carrier gas on the molecular sieve column used to detect H_2, CH_4 and CO. The other three GC columns use UHP He as the carrier gas. CO_2 concentration levels are detected using a porous layer open tubular PLOT-U column. GC sampling occurred approximately every 4 minutes and the TPI/TA was set to control the temperature ramp of the furnace at 10^{o}C/min.

3. Results and Discussion

3.1 Physical Observations. The mass decomposition curve for representative woods, grasses and agricultural residues appears in Figure 2.The largest percent mass loss occurs during pyrolysis between about 275-400^{o}C during which time the biomass structural components depolymerization and condensation reactions. With increasing temperature during low temperature gasification from 400-600^{o}C, the ligno-cellulosic structure evolves into a carbon lattice structure as the pyrolytic char undergoes decomposition and carbonization. Finally, high temperature combustion reactions between 700-850^{o}C continue the char burnout with the aid of oxygen brought in by the steam and oxygen release from the biomass structure itself. By 1000^{o}C all of the biomass samples appear to have completed their mass burnout to residual char and ash. Samples exposed to CO_2 enhanced steam gasification had lower residual char fractions. Two distinct mass decay regimes that correlate with the two distinctly different gas evolution regimes can be identified in the decomposition curve where the transition temperature appears to be in the vicinity of 400^{o}C. The mass decay curves are for a slow gasification rate of 10^{o}C/min and would be significantly different as discussed by Brunner et al. (9) at higher heating rates.

The thermal decomposition of the phenolic and highly crosslinked lignin structure follows a very different set of reaction pathways than that of the polysaccharide cellulose and hemicellulose structures. Lignin decomposition begins much earlier at about 225^{o}C and takes much longer until about 625^{o}C to complete whereas cellulose decomposition begins later at about 325^{o}C and occurs rapidly so that by 425^{o}C decomposition is nearly complete. The behavior of the structural components is manifested in the resultant decomposition behavior of the biomass feedstock. The various feedstocks showed decomposition rates that were intermediate between that of lignin and cellulose though we can expect that residues or grasses high in alkaline content may also exhibit a catalytic effect not present in the decomposition of the pure structural components. To understand the influence of lignin content on the volume of char produced during pyrolysis, the thermal treatment was halted at 400^{o}C following pyrolysis but prior to gasification. Grasses and barks that were lower in lignin content produced chars that were between 20 and 30% less by weight. The distinction between char volumes produced were greatest when comparing samples that involved no CO_2 injection.

Copyright © 2008 by ASME

3.2 Gas Evolution Observations.

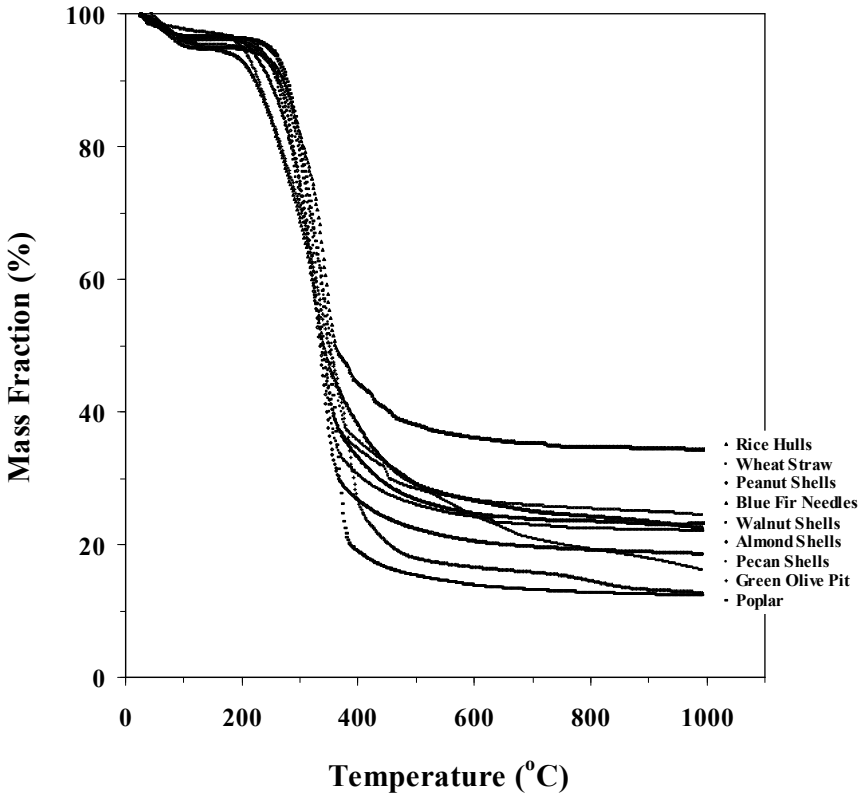

Figure 2. Mass decomposition curve for 0% CO_2

One of the goals of the current study was to understand the impact of CO_2 introduced to enhance the thermal processing of biomass fuels to syngas. The nature of char burnout is distinctly different with CO_2 introduced into the flow stream during steam gasification. Evidence for more complete processing of the fuel is seen in Figures 3-6. Enhanced char burnout was observed for all CO_2 feeds with the woods showing nearly complete char burnout at 30% CO_2. Figure 3 represents 0% CO_2 feed for spruce while Figure 4 shows enhanced char burnout for 10% CO_2 and Figure 5 shows the char resulting from 30% CO_2 steam gasification of spruce. Figure 6 represents 0% CO_2 feed for walnut shells while Figure 7 shows enhanced char burnout to mineral ash for 30% CO_2 steam gasification of walnuts. The mechanism for cellulose pyrolysis Similar to the observations of other investigators, those biomass feedstocks having lower lignin content such as alfalfa (14%), beachgrass (12%), maple bark (19%) and wheat straw (14%) exhibited characteristically smaller char residues than the high lignin feedstocks such as the woods and the needles.

Copyright © 2008 by ASME

Figure 3. Large black char residue from 10% CO_2 spruce steam gasification

Figure 4. Smaller char film from 20% CO_2 spruce steam gasification

Figure 5. Large black char residue from 0% CO_2 walnut shells steam gasification

Figure 6. Small light mineral residue pancake from 30% CO_2 walnut shells steam gasification

In order to better understand the nature of the solid products of combustion, in addition to the volatile species released during gasification of the various biomass feedstocks, several samples were combusted in a furnace in air at atmospheric pressure for 30 minutes at 900^{o}C. Cordgrass and alfalfa that are particularly high in alkaline mineral content were observed to yield the highest combustion mass % residues and were also observed to react with the ceramic glaze of the furnace crucibles. The heat of combustion (HHV) for various fuels was determined using a Parr 1108 Oxygen Bomb Calorimeter. The pelletized samples were combusted under 25 atmospheres of O_2 pressure. Table 1 summarizes the results of the furnace and calorimetry measurements. For those feedstocks whose HHV were not calculated using the calorimeter, database values are presented from either Phyllis ECN (10), BEF (11), SCERP (12), or IIT (13). Calorimetry measurements agree with these and the ORNL (14) and EAFBN (15) database values.

Copyright © 2008 by ASME

Biomass Fuel	Classification	Mass % Residue	HHV (calories/gram)	Cellulose	Hemicellulose	Lignin
Spruce	Softwood	0.338	4719	48	21	28
White Pine	Softwood	0.316	4781	42	21	26
Douglas Fir	Softwood	0.086	4769	41	24	28
Poplar	Hardwood	0.253	4699	41	21	24
Sugar Maple	Hardwood	0.240	4725	39	30	23
Oak	Hardwood	0.110	4782	40	25	26
Alfalfa	Grass	5.890	4338 (10)	30	14	14
Cordgrass	Grass	4.360	4448	43	33	16
Beachgrass	Grass	-	4329	45	31	12
Wheat Straw	Grass	-	4402 (10)	38	29	14
Maple Bark	Bark	4.760	4316	18	33	19
Bl. Fir Needle	Needles	-	4278 (10)	38	24	31
Pine Needle	Needles	4.130	4350 (13)	43	22	38
Gr. Olive Pit	Shell/Pit	-	5165 (10)	-	-	-
Pecan Shell	Shell/Pit	-	4371 (12)	38	23	29
Almond Shell	Shell/Pit	-	4553 (10)	-	-	-
Walnut Shell	Shell/Pit	-	4823 (11)	-	-	-
Peanut Shell	Shell/Pit	-	4732 (11)	36	19	30
Rice Hull	Hull/Husk	-	4575 (10)	6	-	25

Table 1. Furnace Combustion mass % residue, HHV from Calorimetry and databases, and structural composition

In general, the heating values of the dry woods are higher than those of the grasses possessing lower lignin content. The cellulose constituents of a biomass feedstock possess a lower heat content that can be attributed to the water contained within the cellulose structure. High moisture and high mineral content serve as heat sinks that can detract from a feedstock's heating potential. During pyrolysis, the cellulose and hemicellulose structural components are undergoing decomposition into lower heat content gaseous volatiles while the lignin component is undergoing decomposition into a high heat content solid carbonized char structure. The DOE/EERE Biomass database (16) gives an HHV of 4165 cal/gm for wood pulp cellulose and 5062 cal/gm for lignin (wood-derived). Nearly all of the fuels fall within this range. Only green olive pit lies above the lignin value. A possible explanation might be that the high lipid content seed within the pit is raising the total heating value since the net effect of resins and oils is to increase the overall heating value.

The chemical composition of the feedstocks and their combustion and gasification residues were studied using the scanning electron microscope with energy dispersive X-ray spectroscopy equipment of the Materials Research Science and Engineering Center at Columbia. Table 2 presents the weight % results reported by the Princeton Gamma Tech software. Beam energies varying from 5-15 Kev were used to study compositions at different penetration depths. Potassium is seen to give the strongest signal in the energy dispersive X-ray (EDX) spectra. The presence of K and Cl can reduce the ash melting temperature and can account for the corrosion and slagging observed during gasification of herbaceous feedstocks. As expected, the carbon content of unburned woods such as pulverized poplar (91.91% C) was found to be higher than unburned grasses such as alfalfa leaf (79.13% C). The composition change as a result of steam gasification of beachgrass without any CO_2 addition yielded several interesting results. While the C and O levels decreased following gasification, the mineral levels in the char were significantly higher than the raw pulverized beachgrass sample. K rose from 4.99 to 27.23%, Ca from 2.45 to 14.25%, P from 1.31 to 8.69%, Fe from 6.23 to 15.35% and Si from 0.61 to 8.79%. Evidence for the devitrification of the quartz rod and furnace reported by Butterman and Castaldi (17), visible as a marked crackling and crystallization, can be attributed to K_2O that acts as a strong alkaline flux inducing crystalline phase transformations in the silica similar to what occurs in the sintering of pottery glazes. MgO and CaO are highly efficient high temperature fluxes that are also responsible for the highly reactive and embrittling character of herbaceous and residue feedstocks. CO_2 enhanced steam gasification of biomass results in more highly reactive chars not only due to the gasification medium but to catalytic effects resulting from the mineral composition and the levels of K_2O in particular. Senneca (3) found that char combustion and gasification rates were more closely linked to char pore structure. A highly porous network offers increased surface area and a greater number of

Copyright © 2008 by ASME

adsorption sites for the gasifying agents. We observed this correlation between the gasification char porosity and gasification rate. The 0% beachgrass sample exhibited a large black C char that was coated with a white mineral layer of highly variable composition determined by SEM/EDX to be mostly K, Ca and Fe. The carbonization vs. mineralization for varying CO_2 input rates can be explained by the Kawamoto (18) cellulose pyrolysis mechanism in which the major pathway feeding the volatile pyrolysis products into the gasification reactions is the formation of levoglucosan. Either this intermediary is broken down to low molecular weight products with more complete processing and greater gas evolution concentrations in the presence of sufficient O (such as that supplied by the CO_2 input), or polymerization reactions occur to form polysaccharides with high levels of surface carbonization and large quantities of char in the absence of sufficient O or CO. Table 2 presents a weight % analysis for raw pulverized, combusted and gasified samples.

Sample	C	O	K	Na	Mg	Ca	P	Cl	Fe	S	Al	Si
pulverized beachgrass	77.19	2.22	4.99	0.00	0.27	2.45	1.31	2.15	6.23	0.63	0.00	0.61
gasified beachgrass 0% CO2	22.74	0.00	27.23	0.90	1.83	14.25	8.69	0.17	15.35	0.05	0.00	8.79
alfalfa leaf	79.13	8.70	5.29	0.37	0.78	2.77	0.88	1.14	0.00	0.75	0.00	0.19
alfalfa stalk	78.47	8.74	3.26	0.00	0.65	4.88	0.31	2.60	0.00	0.60	0.00	0.49
pulverized Douglas fir	95.96	0.00	0.89	0.00	0.00	0.54	0.02	0.40	0.87	0.47	0.28	0.00
gasified Douglas fir 0% CO2	91.25	7.15	0.04	0.00	0.13	0.11	0.11	0.26	0.00	0.26	0.68	0.00
pulverized maple bark	94.00	2.30	0.79	0.04	0.18	0.00	0.58	0.59	0.00	0.79	0.24	0.47
combusted maple bark	63.94	13.58	0.53	0.00	13.46	0.00	3.54	1.46	0.00	1.98	0.00	1.51
pulverized poplar	91.91	5.84	0.99	0.00	0.08	0.00	0.29	0.00	0.00	0.31	0.32	0.27
combusted poplar	57.82	11.14	2.16	0.00	20.75	0.00	6.85	0.00	0.00	0.76	0.00	0.52

Table 2. SEM/EDX Weight % Analysis of Biomass samples

3.2 Gas Evolution Observations. Figures 7-11 show gas evolution for five representative samples of the biomass feedstocks studied: American beachgrass, oak wood, blue noble fir needles, pecan shells and maple bark. These gas evolution curves are for steam gasification with no CO_2 injection. All of the profiles for woods, grasses and agricultural residues exhibited two distinct gas evolution regimes with a transition temperature in the vicinity of 400^{o}C. H_2 and CO production increase as higher gasification temperatures are reached while CH_4 production remains at low levels throughout the gasification process.

Gas evolution during thermal treatment of biomass, including the kinetics and mechanisms responsible for the temperature profiles of the various volatile species, are strongly governed by free radical reactions. The physical mechanism of char burnout involves surface reactions that can form a protective barrier to impede devolatilization by coating the porous network and thus limiting the internal gas evolution and contact with the gasification medium (H_2O, CO_2).

Degradation of the ligno-cellulosic structure is governed by a collection of coupled mechanisms involving molecular and reactive radical intermediates. The mineral impurities inherent in the biomass feedstock confer a catalytic effect influencing pyrolysis and gasification rates and product selectivity. Subsequent to the initial drying process, initiation reactions begin at 200^{o}C to aid in the lignin decomposition. Initial cleavage reactions produce ring structures containing 5-6 carbons, 2-6 carbon chain fragments and oxygenated species characteristic of the phenolic, aromatic and highly cross-linked phenylpropenoid lignin structural component as well as the 5- and 6-carbon polysaccharide cellulose and hemicellulose structural

Copyright © 2008 by ASME

components. Thermal treatment of hydrocarbon structures is sustained through free radical reactions, with β-carbon bond scission and H abstraction being two of the most important propagation reactions. Also significant, particularly at the onset of the biomass structural decomposition, is the cleavage of the OH radicals from the regularly repeating cellulose chain and the removal of CH_3 radicals from the methoxy groups of the lignin structure.

Though free radical reactions first become significant in the breakdown of the lignin structure above 200°C, they become increasingly more important above 300°C, when OH radicals are being cleaved off of the cellulose backbone at the onset of rapid cellulose decomposition and above 250°C, as CH_3 and H radicals are being released due to H abstraction and β-carbon scission reactions. In addition to the OH radicals released by the cellulose structure, lignin also releases OH radicals in the 250°-400°C temperature range through a β-aryl phenolic elimination mechanism proposed by Kawamoto and Saka (18). In this temperature interval, available CO combines with the OH radicals to produce the increased levels of CO_2 and the depressed levels of CH_4 prior to 400°C that can be observed in Figure 18. This reaction produces H radicals that enter into subsequent propagation reactions responsible for the continual supply of low levels of CH_4 and the rise in H_2 after 500°C visible in Figures 7-14. Alternative pathways proposed by Kawamoto and Saka involving β-aryl and β-ether non-phenolic cleavage of the lignin structure in regime 2 after 400°C, result in fragments that do not include OH radicals that were involved in combination reactions with CO present at lower temperatures. This results in the availability of higher CO concentrations that can either enter into the methanation reactions or be released as CO which is what we are observing in Figures 7-11 and 15-17. With rising temperature, residual carbonyl groups are decarboxylated to CO and CO_2 as the oxygen deficient char (condensed carbon skeleton) strongly adsorbs any available oxygen that includes reactive CO. At higher gasification temperatures, this CO is liberated from the char and appears as an increase in CO gas evolution levels above 500°C. A summary of this behavior for grasses, woods and agricultural residues appears in Figures 15-17.

Banyasz et al. (19) have proposed a set of slow pyrolysis depolymerization reactions that convert an active cellulose structure to tar, char and CO_2 that can account for the rise in CO_2 in the neighborhood of the transition in regimes near 350°-400°C. The alternative pathways proposed by Kawamoto et al.(18) for the slow pyrolysis of cellulose involve either the conversion of levoglucosan to polysaccharides via polymerization reactions that release CO and CO_2 and result in a protective carbonized layer through which further diffusion is impeded or an alternative pathway involving decomposition to low molecular weight volatiles. In this temperature range, radical reactions that include cleavage, decarbonylation and recombination of methylglyoxal and glyceraldehyde release CH_3 radicals and CO molecules. This may help to explain the rise in CO_2 evident at about 325°-375°C seen in Figure18 and the subsequent rise in CO following transition to regime 2 at about 400°C seen in Figures 15-18.

Though CH_4 levels remain consistently low throughout the gasification process, H_2 and CO levels rise with increasing furnace temperature. The decline in H_2 production above 950°C that is summarized for the grasses, woods and agricultural residues in Figures 12-14 appears to be caused by the exhaustion of that portion of the biomass sample that could otherwise have entered into the thermal treatment reactions. Similar behavior was observed by Jangsawang et al. (20,21) with very low concentrations of H_2 and CO below 540°C, increasing levels between 540° and 930°C, and decreasing rates of production of H_2 above 930°C that they attributed solely to competing rates of molecular dissociation and radical formation of H_2.

While many of the high temperature gasification reactions governing hydrocarbon and biomass thermal treatment are similar as the final carbon skeleton is burnt out to char and residual mineral residue, the complex biomass chemical composition results in oxygenated species as well as aromatic and aliphatic fragments that are specific to the ligno-cellulosic structural components. The set of chemical reactions occurring during thermal treatment are highly temperature dependent. Only at very high gasification temperatures (T>700°C) is the endothermic Boudouard reaction

$$C + CO_2 \rightarrow 2CO \qquad \Delta H = +172.5 \text{ kJ/mol}, \qquad (5)$$

the dominant reaction that drives the rising CO levels at high temperature with increasing CO_2 injected into the stream. With rising furnace temperature, the carbon available from the biomass can react with CO_2 contained in the gasification environment. With higher rates of CO_2 injection into the system, the rate of CO production increases with rising temperature. This CO enhancement with CO_2 injection into the steam gasification medium is seen in Figure 20 for beachgrass at T>750°C. CO formation is limited but measurable at low gasification temperatures. The kinetic study by Banyasz et al. involves both a fast high temperature cellulose pyrolysis mechanism releasing CO, CO_2, formaldehyde and hydroxyacetaldehyde that characterized their measurements as well as a slow low temperature cellulose pyrolysis mechanism analogous to our experiment. In this slow pyrolysis pathway tar, char CO_2, H_2O and low molecular weight volatiles, particularly oxygenated species such as aldehydes, are produced that can create biomass-derived CO_2 at

Copyright © 2008 by ASME

low temperatures (T< 700°C) where the Boudouard reaction is not significant and when no CO_2 injection is employed. At lower temperatures the highly reactive biomass char adsorbs any oxygen in the gasification medium including oxygen in the form of CO. Upon further heating, this CO is released following pyrolysis to provide a continuous supply of CO due to desorption above 450°C. The abrupt decline in CO production observed at 30%, 40% and 50% CO_2 injection ratios for steam gasification of beachgrass appearing in Figure 20 is due to exhaustion of the carbon in the sample pan that could be fed into the Boudouard reaction at high gasification temperatures.

The steam reforming reaction becomes a significant reaction above 550°C considering the high dilution rates of the biomass and the relatively high inputs of steam as compared to the concentrations of CO and H_2 that are the preferred high temperature products.

$$C + H_2O \rightarrow CO + H_2$$
$$\Delta H = +131.3 \text{ kJ/mol}, \quad (6)$$

The water gas shift reaction also becomes significant in this transition, between 500°-600°C, from low to high temperature steam gasification

$$CO + H_2O \rightarrow H_2 + CO_2$$
$$\Delta H = -41.2 \text{ kJ/mol}, \quad (7)$$

and is responsible for rising H_2 concentrations in this temperature interval.

Steam in the gasification medium as well as rising temperature are responsible for the increase in H_2 production seen in Figures 12-14 at temperatures above 550°C for the grasses and 650°C for the woods and agricultural residues. At high CO_2 injection ratios, and at higher temperatures above 700°C, the reverse water gas shift reaction combines with the Boudouard reaction to create high CO concentration levels that drive the reverse steam reforming reaction resulting in lower levels of H_2 produced. This H_2 depression during steam gasification of poplar as a result of CO_2 injection can be seen in Figure 21 with discernible H_2 depression occurring for T>750°C.

One pathway of the Demirbas mechanism involves biomass free radical stabilization through H abstraction reactions that cease once the structural component has completed mass decomposition. Though lignin begins a slow decay earlier, cellulose decomposition occurs slightly later and is rapidly completed. This H consumption for stabilization should cease earlier for high cellulosic as compared to high lignitic feedstocks. Since the lignin to cellulose ratio is higher for woods than grasses we would expect a more rapid decomposition in the grasses and a corresponding earlier onset of H_2 production for the grasses as compared to the woods. This behavior can be seen in Figure 12 for the grasses with H_2 production onset beginning about 550°C as compared to Figure 13 for the woods with H_2 production commencing at about 650°C. During pyrolysis the steam introduced for gasification combines with any available CO in the reactor through the water gas shift reaction to produce H_2 that can, through direct hydrogenation methanation reactions,

$$2CO + 2H_2 \rightarrow CH_4 + CO_2$$
$$\Delta H = -246.9 \text{ kJ/mol}, \quad (8)$$

$$CO + 3H_2 \rightarrow CH_4 + H_2O$$
$$\Delta H = -205.7 \text{ kJ/mol}, \quad (9)$$

$$C + 2H_2 \rightarrow CH_4$$
$$\Delta H = -74.4 \text{ kJ/mol}, \quad (10)$$

produce a continuous low level supply of CH_4. In addition to the molecular reactions, radical reactions in which the CH_3 and OCH_3 fragments are cleaved off the phenolic structure are also significant pathways that produce a continuous supply of CH_4 whose rate of production increases in regime 2 as the H_2 and CO levels begin to rise following pyrolysis.

An analogous CO enhancement and H_2 depression is seen in Adsorption Enhanced Steam Reforming (AER) in which CO_2 adsorption rather than injection shifts the gasification reactions and alters the final distribution of gasification products. If injecting large quantities of CO_2 can depress the H_2 production then removal of large quantities should increase the H_2 levels. Similarly if, by removing large quantities of CO_2 through adsorption beds, the CO concentration drops to low levels, then injecting large quantities of CO_2 might be expected to enhance the level of CO production. These observations were made in the AER steam gasification of willow and switchgrass by Alma et al (23). With increasing CO_2 adsorption at about 650°C, a resultant increase in conversion of CO to CO_2 was observed as a result of the water gas shift reaction. As the CO level dropped in their batch reactor, the H_2 level rose abruptly as a result of the CO_2 removal. The AER fixed bed study of Iyer et al. (24,25) showed similar results. As the adsorbent became saturated with CO_2, CO_2 levels abruptly rose just before breakthrough, CO conversion to CO_2 dropped with a rise in CO concentration and a drop in accompnaying H_2 levels.

Several studies have examined the potential of various biomass feedstocks, particularly agricultural and forestry residues, for providing energy and chemicals. The energy potential and seasonal variability in composition of switchgrass, corn stover and wheat straw are discussed in Lee et al. (26). Cool-season, rather than warm-season, grasses were seen to possess lower concentrations of ligno-cellulosic material. New plant growth may need special pretreatment since it contains higher mineral levels than older growth. Using rice hulls

Copyright © 2008 by ASME

rather than rice straw will be less problematic since the levels of K and Cl are much lower so that there will be less of a depression of the ash melting temperature with less damage due to slagging when rice hulls rather than rice straw is used during thermal treatment. Rice hulls are versatile in that they can be used for grinding foodstocks, as animal bedding, as insulation coating during smelting, and as a source of high purity aluminosilicate whiskers and as ash filler for strengthening and coloring of cement as discussed in de Souza et al. (27). The use of three waste fuels: scrap wood, sawdust and pecan shells for cofiring a brick kiln and the nature of the soot, CO and particulates produced were discussed by Stewart and Silcox (28). The need for preheating, grinding the feedstocks and managing the ash residue werre important considerations that need to be addressed before the use of any waste stream can result in a reliable fuel producing a minimally adverse impact on the environment and the process equipment. The study by Chen et al. (29) discusses the differences resulting from water, salt and acid washing and microwave drying pretreatment on the pyrolysis of peanut shells. While washing (deashing) can remove much of the problematic mineral content it can also result in much larger quantities of peanut shell pyrolysis char.

The CO_2 enhanced steam gasification of biomass fuels was extended to the study of Municipal Solid Waste since nearly half of its volume in the United States was found to be biomass in origin. Strategies that would enable a better understanding of the nature of MSW gasification and the values of those operational parameters that could more completely process the waste fuel were seen to include a comparison between the gasification of a representative MSW sample and a variety of biomass feedstocks that included woods, grasses and agricultural residues. We used a suburban residential sample characterizing a winter waste stream that was compiled by a visiting high school student who studied MSW during 2007 using the gasification facilities of the Columbia Combustion and Catalysis lab. More than half of the sample contained starch-based waste, with most of the remainder comprised of paper, plastic and foodstuff. The MSW composite gas evolution curves using no CO_2 injection appear in Figure 19. The gases monitored during steam gasification were H_2, CO, CH_4 and CO_2. For comparison the composite gas evolution from maple wood is shown in Figure 18. A comparison of the two graphs shows that the mole fractions of the various gasification products that were monitored are close in value and the nature of their temperature dependent evolution profiles is similar indicating that studying biomass gasification can aid in understanding the steam gasification of MSW fuels.

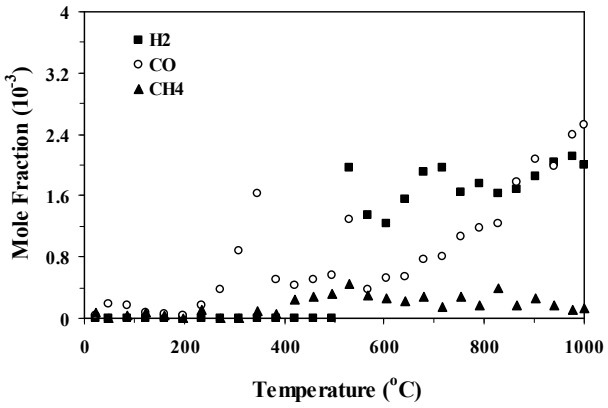

Figure 7. 0% CO_2 Beachgrass Composite Gas Evolution

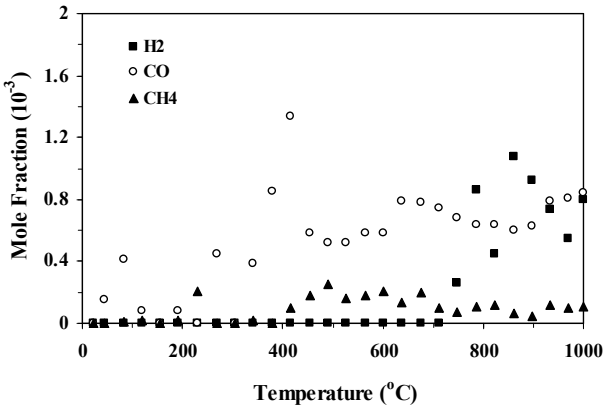

Figure 8. 0% CO_2 Oak Composite Gas Evolution

Copyright © 2008 by ASME

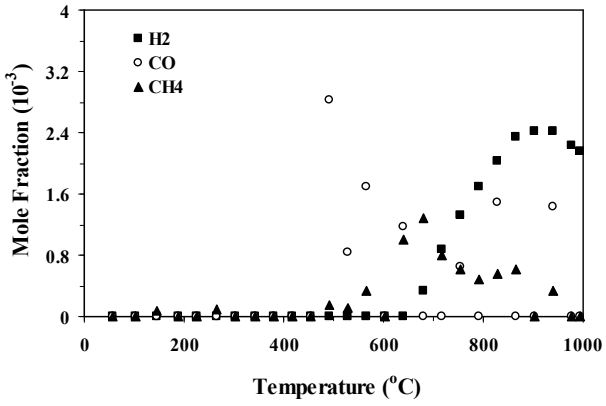

Figure 9. 0% CO_2 Blue Fir Needle Composite Gas Evolution

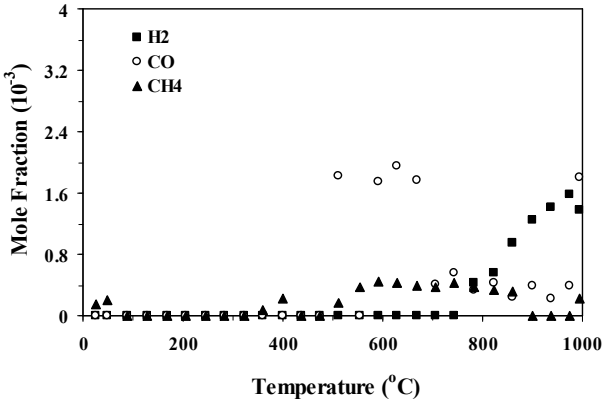

Figure 10. 0% CO_2 Pecan Shell Composite Gas Evolution

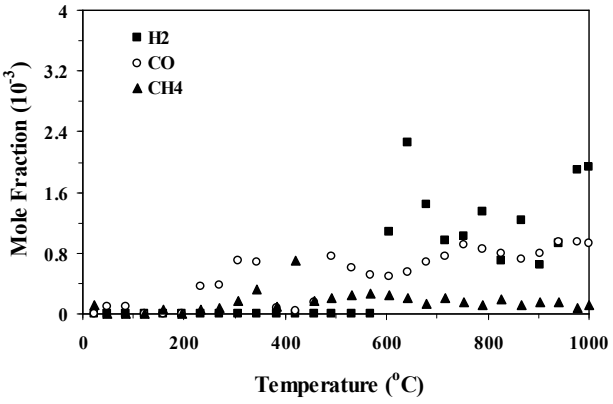

Figure 11. 0% CO_2 Maple Bark Composite Gas Evolution

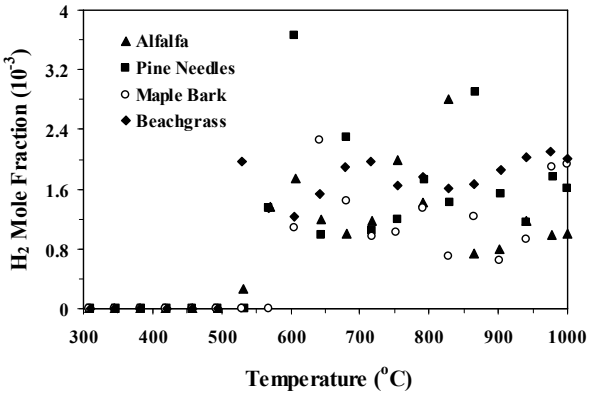

Figure 12. 0% CO_2 Grasses Composite H2 Gas Evolution

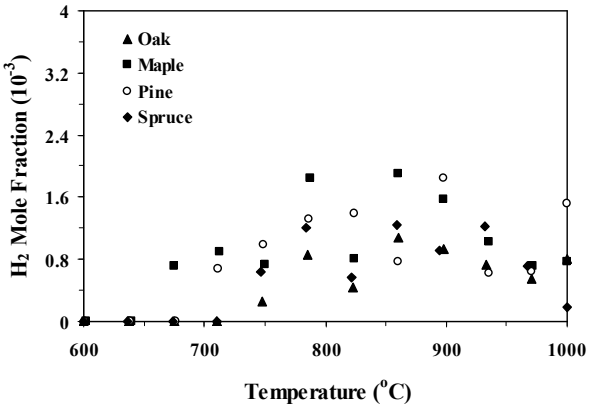

Figure 13. 0% CO_2 Woods Composite H2 Gas Evolution

Copyright © 2008 by ASME

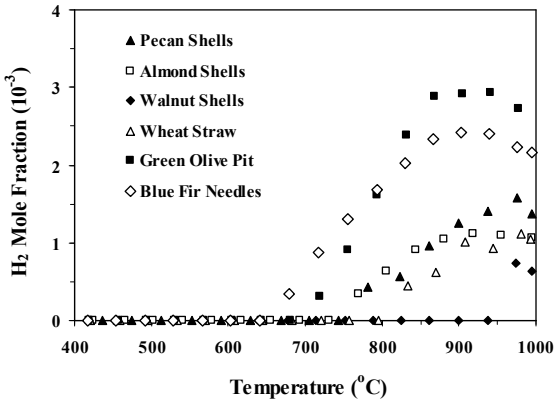

Figure 14. 0% CO_2 Agricultural Residues Composite H2 Gas Evolution

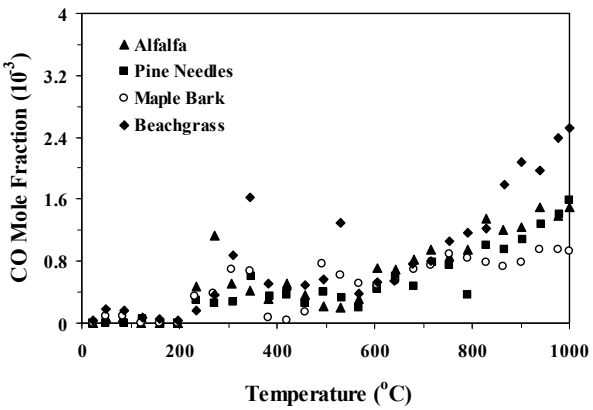

Figure 15. 0% CO_2 Grasses Composite CO Gas Evolution

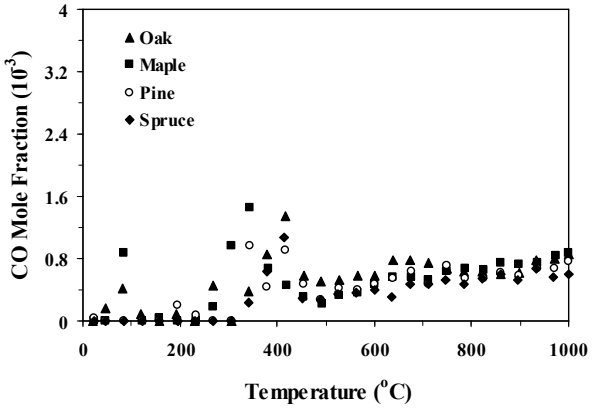

Figure 16. 0% CO_2 Woods Composite CO Gas Evolution

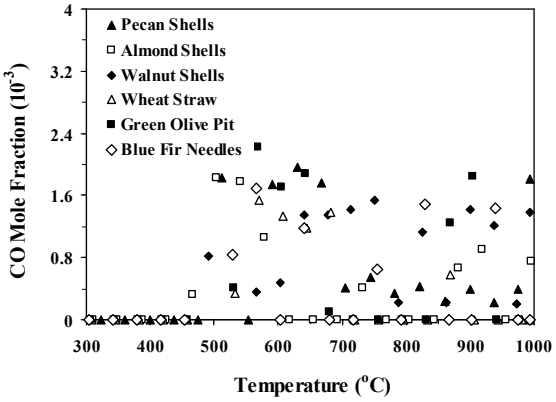

Figure 17. 0% CO_2 Agricultural Residues Composite CO Gas Evolution

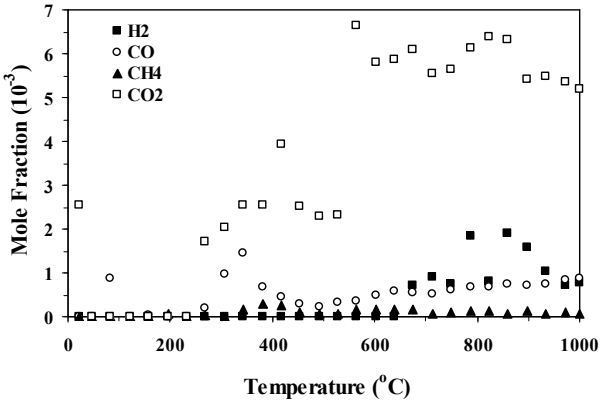

Figure 18. 0% CO_2 Maple Wood Composite Gas Evolution

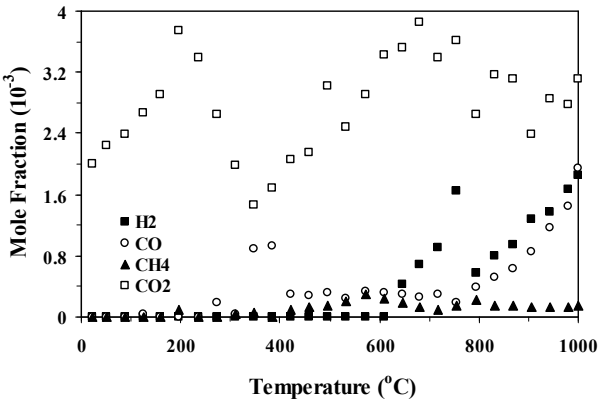

Figure 19. 0% CO_2 MSW Winter Sample Composite Gas Evolution

Copyright © 2008 by ASME

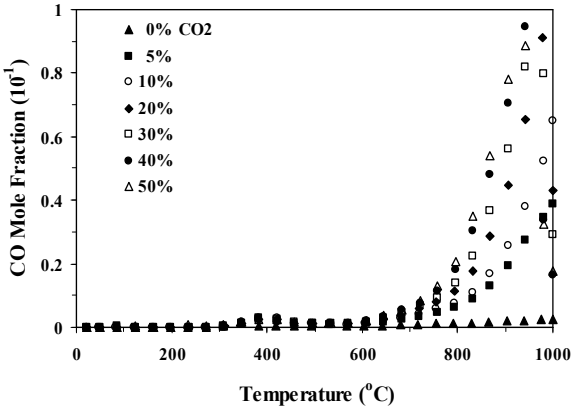

Figure 20. CO Evolution from Beachgrass showing CO Enhancement with CO_2 for T > 750°C

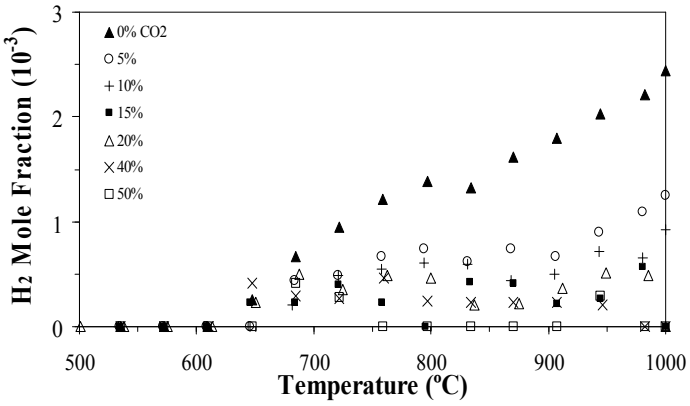

Figure 21. H_2 Evolution from Poplar showing H_2 Depression with CO_2 for T > 750°C

4. Conclusion

The current study represents a series of steam gasification tests performed on a variety of biomass feedstocks that included grasses, woods and agricultural residues. A comparison in gas evolution profiles was made to show the similarities between the gasification products of biomass and MSW. Varying concentrations of CO_2 were introduced into the feed stream to assess the impact on species concentrations as a result of CO_2 injection during the steam gasification of biomass. Two distinct regimes whose transition was in the vicinity of 400°C showed distinctly different mass decomposition rates and gas evolution profiles. The majority of the feedstock mass decomposition occurred between 250°-200°C. Large pyrolysis char volumes correlated well with higher lignin compositions. Evidence that CO_2 injection can aid in char burnout was seen by observing the volumes of char or mineral ash remaining in the sample pan following CO_2 enhanced steam gasification.

H_2 concentrations become measurable for the woods and agricultural residues after 650°C while for the grasses they can be detected by 550°C. As the furnace temperature increases, steam reforming and H radical addition account for rising H_2 levels during gasification. Above 600°C, steam reforming, the Boudouard reaction, the reverse water gas shift reaction and burnout of the char structure all contribute to the rising CO levels with temperature. In the vicinity of the transition temperature between regimes at about 400°C molecular methanation reactions fed by increasing levels of CO and H_2 as well as free radical reactions involving cleavage of CH_3 radicals from the lignin structure result in rising levels of methane that are maintained at continuous low levels. CO_2 injection into the feed stream results in enhanced levels of CO above 750°C and depressed levels of H_2 above 750°C.

References

1. U.S. Dept. of Energy, EERC Biomass Program, Biomass as Feedstock for a Bioenergy and Bioproducts Industry: The Technical Feasibility of a Billion-Ton Annual Supply, April 2005

2. Nehrozoglu, A., Foster Wheeler Power Group Inc., Advanced CO_2 Cycle Power Generation, Technical Progress Report, U.S. DOE Contract: DE-FC26-02NT41621, January 2004

3. Senneca, O., Kinetics of pyrolysis, combustion and gasification of three biomass fuels, Fuel Processing Technology, Volume 88, pp. 87-97, 2007

4. Minkova, V., S.P. Marinov, R. Zanzi, E. Bjornbom, T. Budinova, M. Stefanova, and L. Lakov, Thermochemical treatment of biomass in a flow of steam or in a mixture of steam and carbon dioxide, Fuel Processing Technology, Volume 62, pp. 45-52, 2000

5. Butterman, H.C., and M.J. Castaldi, Influence of CO_2 Injection on Biomass Gasification, Ind. Eng. Chem. Res., Volume 46, pp. 8875-8886, 2007

6. Ochoa, J., M.C. Cassanello, P.R. Bonelli, and A.L. Cukierman, CO_2 gasification of Argentinian coal chars: a kinetic characterization, Fuel Processing Technology, Volume 74, pp. 161-176, 2001

Copyright © 2008 by ASME

7. Ye, D.P., J.B. Agnew and D.K. Zhang, Gasification of a South Australian low-rank coal with carbon dioxide and steam: kinetics and reactivity studies, Fuel, Volume 77, pp. 1209-1219, 1998

8. Demirbas, A., Production and Characterization of Bio-Chars from Biomass via Pyrolysis, Energy Sources, Part A: Recovery, Utilization and Environmental Effects, Volume 28, pp. 413-422, 2006

9. Brunner, P.H., and P.V. Roberts, The Significance of Heating Rate on Char Yield and Char Properties in the Pyrolysis of Cellulose, Carbon, Volume 18, pp. 217-224, 1980

10. The Phyllis biomass database of the Energy Research Center of the Netherlands, www.ecn.nl/phyllis/

11. Biomass Energy Foundation: Proximate/Ultimate Analysis http://www.woodgas.com/proximat.htm (accessed 2008)

12. Stewart, E.S., and G.D. Silcox, Selection and Analysis of the Use of Alternative Fuels in Brick Manufacturing, pp. 1-24, SCERP Project Number: AQ95-9, 1999 http://www.scerp.org/projects/AQ95_9.html

13. Safi, M.J., I.M. Mishra and B. Prasad, Global degradation kinetics of pine needles in air, Thermochimica Acta, Volume 412, pp. 155-162, 2004

14. Oak Ridge National Laboratory, Bioenergy Feedstock Development Programs http://bioenergy.ornl.gov/papers/misc/biochar_factsheet.html (accessed 2008)

15. European Agriculture and Forestry Biomass Network: http://www.vtt.fi/virtual/afbnet/ (accessed 2008)

16. U.S. Dept. of Energy Biomass Program- Biomass Feedstock Composition and Property Database http://www1.eere.energy.gov/biomass/feedstock_databases.html (accessed 2008)

17. Butterman, H.C., and M.J. Castaldi, Hydrogen Production via Gasification of Biomass Fuels, 26th International Conference on Incineration and Thermal Treatment Technologies (IT3), Phoenix AZ, May 2007

18. Kawamoto, H., M. Murayama, and S. Saka, Pyrolysis behavior of levoglucosan as an intermediate in cellulose pyrolysis: polymerization into polysaccharide as a key reaction to carbonized product formation, J. of Wood Science, Volume 49, pp. 469-473, 2003

19. Banyasz, J.L., S. Li, J. Lyons-Hart, and K.H. Shafer, Gas evolution and the mechanism of cellulose pyrolysis, Fuel, Volume 80, p.1757-1763, 2001

20. Jangsawang W., A.K. Gupta, K. Kitagawa, and S.C. Lee, High Temperature Steam and Air Gasification of Non-Woody Biomass Wastes, 2nd Joint International Conference on Sustainable Energy and Environment, November 2006, Thailand

21. Jangsawang W., A. Klimanek, and A.K. Gupta, Enhanced Yield of Hydrogen From Wastes Using High Temperature Steam Gasification, J. of Energy Resources Technology, Volume 128(3), pp. 179-185, September 2006

22. Demirbas, A., Mechanisms of liquefaction and pyrolysis reactions of biomass, J. of Energy Conversion & Management, Volume 41, pp. 633-646, 2000

23. Alma, M.H., O. Cinar, and H.R. Oz, Zero-Emission Method for Hydrogen Production, International Hydrogen Energy Congress and Exhibition, Istanbul Turkey, July 2005

24. Iyer, M., S. Ramkumar, and L.S. Fan, Enhanced H_2 Production Integrated with CO_2 Separation in a Single-Stage, DOE Annual Report, Contract No. DE-FC26-03NT41853, October 2006

25. Iyer, M., S. Ramkumar, and L.S. Fan, High Purity H_2 Production with in-situ CO_2 and Sulfur Capture, A.I.Chem.E. Annual Conference, 2006

26. Lee, D.K., V.N. Owens, A. Boe, and P. Jeranyama, Composition of Herbaceous Feedstocks, South Dakota State University, Sun Grant Initiative http://agbiopubs.sdstate.edu/articles/SGINC1-07.pdf

27. de Souza, M.F., P.S. Batista, I. Regiani, J.B.L. Liborio, and D.P.F. de Souza, Rice Hull-Derived Silica: Applications in Portland Cement and Mullite Whiskers, Materials Research, Volume 3 No. 2, pp. 1-12, 2000

28. Chen, H. F. Xin, X. Wang, H. Yang, and J. Wang, Novel pretreatments for peanut shell pyrolysis, Huazhong University State Key Lab of Coal Combustion, 2004 http://frc.kier.re.kr/down/P1-6.pdf

Copyright © 2008 by ASME